Constraining inflationary dark matter in the luminogenesis model

Pham Q. Hung[a,b] and Kevin J. Ludwick[a]

Department of Physics, University of Virginia,
Charlottesville, VA, 22904-4714 U.S.A.

Center for Theoretical and Computational Physics, Hue University College of Education,
34 Le Loi Street, Hue, Vietnam

E-mail: pqh@virginia.edu, kludwick@virginia.edu

Abstract. Using renormalization-group flow and cosmological constraints on inflation models, we exploit a unique connection between cosmological inflation and the dynamical mass of dark matter particles in the luminogenesis model, a unification model with the gauge group $\mathrm{SU}(3)_C \times \mathrm{SU}(6) \times \mathrm{U}(1)_Y$, which breaks to the Standard Model with an extra gauge group for dark matter when the inflaton rolls into the true vacuum. In this model, inflaton decay gives rise to dark matter, which in turn decays to luminous matter in the right proportion that agrees with cosmological data. Some attractive features of this model include self-interacting dark matter, which may resolve the problems of dwarf galaxy structures and dark matter cusps at the centers of galaxies.

Contents

1 Introduction

Dark matter comprises a large portion of our universe, and yet it still eludes our full comprehension. There are many unsolved mysteries about the nature of dark matter, such as the "missing satellite" problem and the dark matter cusps at the centers of galaxies found in simulations but not in observations.

What if all matter originally came from the dark sector? One possible way to combine dark matter and the Standard Model is via the luminogenesis model [1, 2]. It is a model that undergoes the symmetry breaking $SU(3)_C \times SU(6) \times U(1)_Y \to SU(3)_C \times SU(4)_{DM} \times SU(2)_L \times U(1)_Y \times U(1)_{DM}$ at the DUT (Dark Unified Theory) scale. This breaking occurs when the inflaton slips into the true vacuum of its potential. The inflaton decays to dark matter, while decay to luminous matter is suppressed at the tree level. Below the luminogenesis scale M_{lum}, dark matter decays to radiation and mirror matter [3] (which will be discussed below), and almost all mirror fermions decay to standard fermions. Freeze-out of these conversions occurs at high energy scales, leaving standard Big Bang Nucleosynthesis unaffected. In this model, $SU(4)_{DM}$ is unbroken and is confining at a scale much smaller than the DUT scale. This is the main emphasis of this manuscript.

Dark matter in this model is self-interacting, which may resolve the discrepancies between observations and simulations mentioned above. Another attractive feature of this model is the absence of proton decay, which may explain its lack of observation.

In this paper, we explore the interesting and unique connection between cosmic inflation and dark matter. We first analyze renormalization-group flow from the DUT scale to the confinement scale of $SU(4)_{DM}$, which provides the dynamical mass of the dark matter particles. We obtain the $SU(4)_{DM}$ coupling at the DUT scale from the unification with the $SU(2)_L$ coupling at the DUT scale, which we get from running the $SU(2)_L$ coupling from the electroweak scale to that scale. Then we examine constraints on the DUT scale based on constraints on inflation from Planck for a symmetry-breaking (Coleman-Weinberg) inflation potential and obtain constraints on the dark matter dynamical mass.

Before embarking on the main topic of this manuscript, namely the connection between cosmic inflation and dark matter, it is important, for the sake of clarity, to give a short summary of the luminogenesis model [1, 2] and of the electroweak-scale right-handed neutrino model (EWν_R model) [3] where mirror fermions appear.

2 Mini-review of the luminogenesis model and the EWν_R model

The model proposed by [1, 2] which incorporates the EWν_R model [3, 4] can be summarized as follows.

The idea in [1, 2] was to unify the dark matter and luminous sectors into a gauge group, SU(6), which contains the Standard Model (SM) SU(2)$_L$ under which dark matter particles are singlets and SU(4), the DM gauge group which confines at some scale Λ_4. In this model, SU(3)$_C$ and U(1)$_Y$ are just "spectator" gauge groups. Specifically, we have (with the acronym DUT referring to that type of unification)

$$\mathrm{SU(3)}_C \times \mathrm{SU(6)} \times \mathrm{U(1)}_Y \xrightarrow{M_{\mathrm{DUT}}} \mathrm{SU(3)}_C \times \mathrm{SU(4)}_{\mathrm{DM}} \times \mathrm{SU(2)}_L \times \mathrm{U(1)}_{\mathrm{DM}} \times \mathrm{U(1)}_Y, \quad (2.1)$$

$$\mathrm{SU(3)}_C \times \mathrm{SU(4)}_{\mathrm{DM}} \times \mathrm{SU(2)}_L \times \mathrm{U(1)}_{\mathrm{DM}} \times \mathrm{U(1)}_Y \xrightarrow{\Lambda_{\mathrm{DM}}} \mathrm{SU(3)}_C \times \mathrm{SU(4)}_{\mathrm{DM}} \times \mathrm{SU(2)}_L \times \mathrm{U(1)}_Y, \tag{2.2}$$

$$\mathrm{SU(3)}_C \times \mathrm{SU(4)}_{\mathrm{DM}} \times \mathrm{SU(2)}_L \times \mathrm{U(1)}_Y \xrightarrow{\Lambda_{\mathrm{EW}}} \mathrm{SU(3)}_C \times \mathrm{SU(4)}_{\mathrm{DM}} \times \mathrm{U(1)}_{em}. \tag{2.3}$$

As one can see from the above symmetry breaking pattern, the Luminogenesis model contains two unbroken non-abelian gauge groups: SU(3)$_C$ and SU(4)$_{\mathrm{DM}}$, both of which are assumed to confine at Λ_{QCD} and Λ_4 respectively. The aim of this paper is to determine what Λ_4 (replaced by the symbol μ_{DM} for convenience below) might be since this scale is related to the dynamical mass of dark matter. To complete this mini-review, we will list the fermion and scalar representations and summarize their roles in the Luminogenesis model.

In [1, 2], a set of criteria was written down to guide the choice of fermion representations.

1) SM particles are required to be singlets under the DM gauge group SU(4)$_{\mathrm{DM}}$. In particular, left-handed SM particles are required to be doublets under SU(2)$_L$. From table 1, one can see that the $\underline{6}$ representation of SU(6) satisfies this criterion since it contains $(\mathbf{1}, \mathbf{2})$ under SU(4) × SU(2). A representation under SU(3)$_C$ × SU(6) × U(1)$_Y$ which contains the SM left-handed quark doublets and right-handed quark singlets is then represented by $(\mathbf{3}, \mathbf{6}, \mathbf{1/6})_{\mathbf{L}} + (\mathbf{3}, \mathbf{1}, \mathbf{2/3})_{\mathbf{R}}$ with the last entries being the U(1)$_Y$ quantum number. Similarly, the SM leptons are contained in $(\mathbf{1}, \mathbf{6}, -\mathbf{1/2})_{\mathbf{L}} + (\mathbf{1}, \mathbf{1}, -\mathbf{1})_{\mathbf{R}}$.

2) Since the gauge group at the DUT is SU(3)$_C$ × SU(6) × U(1)$_Y$ and $\underline{6}$ is a complex representation, anomaly freedom requires that for every left-handed fermion multiplet there exists an equivalent right-handed multiplet so that the anomaly cancels between left and right. The right-handed SU(2) doublets and left-handed singlets are called "mirror fermions" in [3]. They are contained in $(\mathbf{3}, \mathbf{6}, \mathbf{1/6})_{\mathbf{R}} + (\mathbf{1}, \mathbf{6}, -\mathbf{1/2})_{\mathbf{R}} + (\mathbf{3}, \mathbf{1}, \mathbf{2/3})_{\mathbf{L}} + (\mathbf{1}, \mathbf{1}, -\mathbf{1})_{\mathbf{L}}$. The introduction of the mirror fermions in [3] was motivated by the possibilities of having Majorana masses for right-handed neutrinos of the order of the electroweak scale, i.e. $O(\Lambda_{\mathrm{EW}} \sim 246\,\mathrm{GeV})$ naturally and of the possible detection of these right-handed neutrinos directly at the Large Hadron Collider (LHC). This would yield a direct test of the seesaw mechanism which provides an elegant explanation for the smallness of neutrino masses. Details of the EWν_R model can be found in [3, 4].

As discussed in [1, 2], by embedding the SM gauge group SU(2) into SU(6), the existence of these mirror fermions comes out naturally from the requirement of anomaly freedom of SU(3)$_C$ × SU(6) × U(1)$_Y$. Extensive studies of the contributions of mirror fermions to electroweak precision parameters have been carried out in [4] with the conclusion that the EWν_R model fits the data very well despite the presence of right-handed mirror fermions.

SU(6)	$\mathrm{SU(4)_{DM} \times SU(2)_L \times U(1)_{DM}}$
6	$(\mathbf{1,2})_{\mathbf{2}} + (\mathbf{4,1})_{-\mathbf{1}}$
20	$(\mathbf{4,1})_{\mathbf{3}} + (\mathbf{4^*,1})_{-\mathbf{3}} + (\mathbf{6,2})_{\mathbf{0}}$
35	$(\mathbf{1,1})_{\mathbf{0}} + (\mathbf{15,1})_{\mathbf{0}} + (\mathbf{1,3})_{\mathbf{0}} + (\mathbf{4,2})_{-\mathbf{3}}$
	$+(\mathbf{4^*,2})_{\mathbf{3}}$

Table 1. $(\mathbf{1,2})_{\mathbf{2}}$ represents luminous matter while $(\mathbf{4,1})_{\mathbf{3}} + (\mathbf{4^*,1})_{-\mathbf{3}}$ represent dark matter.

Mirror quarks and leptons can be searched for at the LHC [5]. The search for the electroweak-scale right-handed neutrinos is particularly interesting since it will be a direct test of the seesaw mechanism. As emphasized in [3], the production of $\nu_R\nu_R$ at the LHC can give rise to interesting signals such as like-sign dileptons. Furthermore, the lightest mirror quark can decay into a SM quark by emitting a SM-singlet Higgs scalar ($q_R^M \to q_L + \phi_S$) through an interaction Lagrangian of the form: $g_{Sq}\,\bar{q}_L\,\phi_S\,q_R^M + $ h.c. where q_L and q_R^M refer to a SM left-handed and mirror right-handed quark doublet respectively. A similar decay process applies to the lightest mirror lepton ($l_R^M \to l_L + \phi_S$) with $g_{Sl}\,\bar{l}_L\,\phi_S\,l_R^M + $ h.c.

Why would we be interested in the decays of mirror fermions into SM fermions? First, this would be an important process by which we can detect mirror fermions at colliders such as the LHC. Second, as expounded in [2], dark matter (denoted by χ) is contained in the **20** and the inflaton is the singlet part of **35** (see table 1). Since $\mathbf{20 \times 20 = 1_s + 35_a + 175_s + 189_a}$, the inflaton decays mainly into dark matter through the interaction $g_{20}\,\Psi_{20}^T\sigma_2\Psi_{20}\,\phi_{35}$ which contains $g_{20}\,\chi_L^T\sigma_2\chi_L^c\phi_{\mathrm{inf}}$. (This is one of the main points of [2]: the predominance of dark over luminous matter.) The conversion of a fraction of dark matter to luminous matter is achieved through the interactions with two scalar fields: $\Phi_{15}^{(L)}$ and $\Phi_{\bar{15}}^{(R)}$, and given by $\frac{g_6^2}{M_{15}^2}\,(\chi_L^T\sigma_2 l_L)\,(\chi_L^{c,T}\sigma_2 l_L^{M,c}) + $ h.c., resulting in $\chi_L + \chi_R \to l_L + l_R^M$ and $\bar{\chi}_L + \bar{\chi}_R \to \bar{l}_L + \bar{l}_R^M$. Although the decay length of the process $l_R^M \to l_L + \phi_S$ could be macroscopic at the LHC ("long-lived" l_R^M), in the early universe, l_R^M basically decays promptly into SM leptons. This, in a nutshell, is what [2] refers to as "luminogenesis". How effective the conversion of dark matter into SM particles is a question that depends on the prefactor $\frac{g_6^2}{M_{15}^2}$.

As is noted in [2], a small dark matter asymmetry $\Delta n_\chi = n_\chi - n_{\bar{\chi}}$ is assumed to be present, with $n_\chi = n_{\mathrm{sym}} + \Delta n_\chi$ only slightly bigger than $n_{\bar{\chi}} = n_{\mathrm{sym}}$, where n_{sym} is the symmetric part of n_χ and $n_{\bar{\chi}}$. The asymmetric part consists of the small excess $\Delta n_\chi \ll n_{\mathrm{sym}}$. We assume that there is a global $\mathrm{U(1)}_\chi$ symmetry for dark matter. The interactions involving the gauge bosons of the coset group $\mathrm{SU(6)/\,SU(4)\times SU(2)\times U(1)_{DM}}$ explicitly break the $\mathrm{U(1)}_\chi$ symmetry, and their decays involving the interferences between the tree-level and one-loop diagrams will ultimately produce a net DM number, assuming the presence of CP violation in the DM sector. (This process is similar to the one involving X and Y gauge bosons in SU(5) GUT Theory.) χ and $\bar{\chi}$ can annihilate via γ_{DM}, the massive dark photon of $\mathrm{U(1)_{DM}}$, into luminous particle-antiparticle pairs via the effective interaction $\frac{g^2}{M_{\gamma_{\mathrm{DM}}}}(\bar{\chi}\gamma_\mu\chi)(\bar{f}\gamma^\mu f)$, and the particle-antiparticle pairs of luminous fermions annihilate to radiation. The coefficients for this annihilation process and the conversion process involving the aforementioned scalars $\Phi_{15}^{(L)}$ and $\Phi_{\bar{15}}^{(R)}$ are independent of each other, and they are such that 14% of all dark matter (14% of asymmetric and symmetric parts) converts via the scalars and 86% of asymmetric and symmetric parts annihilates via γ_{DM} ultimately to radiation. The 14% of the symmetric parts of n_χ and $n_{\bar{\chi}}$ that is converted to luminous matter via the scalars has equal parts of

luminous particles and anti-particles, and these annihilate to radiation. So the whole of the symmetric parts of n_χ and $n_{\bar\chi}$ is mainly converted to radiation. But since annihilation via $\gamma_{\rm DM}$ requires the presence of both χ and $\bar\chi$, this annihilation does not affect the asymmetric part Δn_χ, so overall, we are left with radiation from the symmetric parts of n_χ and $n_{\bar\chi}$ and 14% luminous matter and 86% DM in the asymmetric part, giving the correct proportion of luminous to dark matter as the conversion process via the scalars freezes out. So we see that this process of luminogenesis depends upon both freeze-out and asymmetry in dark matter (and the asymmetry is propagated through to luminous matter), and the coefficients of the processes discussed are such that luminogenesis gives what is observationally expected. These processes involved in luminogenesis are discussed in more detail in [2].

Notice that, in principle, the **15** and **$\overline{15}$** scalars could mix with the scalar **35** (which contains the inflaton) of the form $\lambda_{15,35}\mathbf{15}\times\overline{\mathbf{15}}\times\mathbf{35}\times\overline{\mathbf{35}}$. We assume that $\lambda_{15,35}$ is small enough that such a mixing does not affect the inflationary potential and other physical processes discussed in [2]. It is however interesting to study consequences, if any, of such a mixing but this is beyond the scope of this paper.

3 Predictions for the dark matter dynamical mass from RG flow

Combining renormalization-group (RG) flow with constraints on cosmic inflation from Planck [6, 7], we can make a prediction for the dark matter dynamical mass. As discussed in [1, 2], $\mathrm{SU}(6)\to\mathrm{SU}(4)_{\rm DM}\times\mathrm{SU}(2)_L\times\mathrm{U}(1)_{\rm DM}$. The β-function equation for $\mathrm{SU}(N)$, ignoring the negligible term for the contribution due to scalar fields, is

$$\frac{d\alpha}{d\ln\mu}\equiv\beta(\alpha)=-\left[\frac{11}{3}N-\frac{2}{3}C(R)n_{f_L}-\frac{2}{3}C(R)n_{f_R}\right]\frac{\alpha^2}{2\pi}+O(\alpha^3),\qquad(3.1)$$

where the second and third terms correspond to the contributions from left-handed and right-handed fermions respectively.

The representations and group structure of the luminogenesis model for each of the three families are given below [2]. In passing, the existence of mirror fermions, as proposed by [3], provides a mechanism in which right-handed neutrinos obtain Majorana masses proportional to the electroweak scale, and they could be searched for at the Large Hadron Collider.

The inflaton is represented by $(\mathbf{1},\mathbf{1})_\mathbf{0}$ of **35**. It is assumed that $(\mathbf{15},\mathbf{1})_\mathbf{0}+(\mathbf{1},\mathbf{3})_\mathbf{0}$ $+(\mathbf{4},\mathbf{2})_{-\mathbf{3}}+(\mathbf{4^*},\mathbf{2})_\mathbf{3}$ of **35** have masses that are on the order of the DUT scale and are therefore not included in our analysis of RG flow. The inflaton decays to dark matter through a coupling via $\mathbf{20}\times\mathbf{20}=\mathbf{1_s}+\mathbf{35_a}+\mathbf{175_s}+\mathbf{189_a}$, while decay to luminous matter is suppressed at the tree level. Dark matter can decay to luminous matter through a coupling via $\mathbf{20}\times\bar{\mathbf{6}}=\mathbf{15}+\mathbf{105}$ and $\mathbf{20}\times\mathbf{6}=\overline{\mathbf{15}}+\overline{\mathbf{105}}$ and through the massive gauge boson of $\mathrm{U}(1)_{\rm DM}$, the dark photon. More details are in [2].

The $\mathrm{SU}(4)_{\rm DM}$ dark matter fermions are represented by $(\mathbf{4},\mathbf{1})_\mathbf{3}+(\mathbf{4^*},\mathbf{1})_{-\mathbf{3}}$ in the **20** representation of $\mathrm{SU}(6)$. The $(\mathbf{6},\mathbf{2})_\mathbf{0}$ part of **20** is assumed to decouple below its mass scale M_2. Since dark matter should have no $\mathrm{U}(1)_Y$ charge, the $\mathrm{SU}(4)_{\rm DM}$ particles in $(\mathbf{4},\mathbf{1})_{-\mathbf{1}}$ in the **6** representation of $\mathrm{SU}(6)$ cannot be dark matter, and they are assumed to decouple below the mass scale M_1.

For $\mathrm{SU}(2)_L$, the Casimir factor for the representation R for all the right-handed and left-handed contributions is $C(\mathbf{2})=\frac{1}{2}$. The numbers of right- and left-handed fermions are $n_{f_R}=n_{f_L}=(3+1)3=12$ for scales $\mu<M_2$ because, using tables 1 and 2, we see that $(\mathbf{3},\mathbf{6},\mathbf{1/6})_{L,R}$ is $(\mathbf{3},\mathbf{1},\mathbf{2},\mathbf{1/6})_{L,R}+(\mathbf{3},\mathbf{4},\mathbf{1},\mathbf{1/6})_{L,R}$ under $\mathrm{SU}(3)\times\mathrm{SU}(4)_{\rm DM}\times\mathrm{SU}(2)_L\times\mathrm{U}(1)_Y$

	$\mathrm{SU}(3)_c \times \mathrm{SU}(6) \times \mathrm{U}(1)_Y$
R ⊃ SM fermions	$(\mathbf{3}, \mathbf{6}, \mathbf{1/6})_\mathbf{L} + (\mathbf{1}, \mathbf{6}, -\mathbf{1/2})_\mathbf{L}$
	$+(\mathbf{3}, \mathbf{1}, \mathbf{2/3})_\mathbf{R} + (\mathbf{3}, \mathbf{1}, -\mathbf{1/3})_\mathbf{R}$
	$+(\mathbf{1}, \mathbf{1}, -\mathbf{1})_\mathbf{R}$
R ⊃ mirror fermions	$(\mathbf{3}, \mathbf{6}, \mathbf{1/6})_\mathbf{R} + (\mathbf{1}, \mathbf{6}, -\mathbf{1/2})_\mathbf{R}$
	$+(\mathbf{3}, \mathbf{1}, \mathbf{2/3})_\mathbf{L} + (\mathbf{3}, \mathbf{1}, -\mathbf{1/3})_\mathbf{L}$
	$+(\mathbf{1}, \mathbf{1}, -\mathbf{1})_\mathbf{L}$
R ⊃ dark matter fermions	$(\mathbf{1}, \mathbf{20}, \mathbf{0})$

Table 2. R in the left column denotes representation. Standard Model (SM) left-handed doublets and right-handed singlets comprise the first row, mirror right-handed doublets [3] and left-handed singlets comprise the second row, and dark matter left- and right-handed fermions belong to the last row.

and it contains three $\mathrm{SU}(2)_L$ doublets (due to color) per family, and $(\mathbf{1}, \mathbf{6}, -\mathbf{1/2})_{L,R}$, which is $(\mathbf{1}, \mathbf{1}, \mathbf{2}, -\mathbf{1/2})_{L,R} + (\mathbf{1}, \mathbf{4}, \mathbf{1}, -\mathbf{1/2})_{L,R}$ under $\mathrm{SU}(3) \times \mathrm{SU}(4)_{\mathrm{DM}} \times \mathrm{SU}(2)_L \times \mathrm{U}(1)_Y$, contains one $\mathrm{SU}(2)_L$ doublet per family. When $\mu > M_2$, we have an additional (left-handed) contribution to the number of fermions of $6 \cdot 3 = 18$ from the six $\mathrm{SU}(2)_L$ doublets per family from $(\mathbf{6}, \mathbf{2})_\mathbf{0}$. Therefore, following equation (3.1), the $\mathrm{SU}(2)_L$ one-loop β-function is $\beta_2(\alpha_2) = -f_2 \frac{\alpha_2^2}{2\pi}$, where

$$f_2^{\mu < M_2} = \left(\frac{11}{3} \cdot 2 - \frac{2}{3} \cdot \frac{1}{2} \cdot 12 - \frac{2}{3} \cdot \frac{1}{2} \cdot 12 \right) = -\frac{2}{3},$$

$$f_2^{\mu > M_2} = \left(\frac{11}{3} \cdot 2 - \frac{2}{3} \cdot \frac{1}{2} \cdot 12 - \frac{2}{3} \cdot \frac{1}{2} \cdot 12 - \frac{2}{3} \cdot \frac{1}{2} \cdot 18 \right) = -\frac{20}{3}. \tag{3.2}$$

For $\mathrm{SU}(4)_{\mathrm{DM}}$, $C(\mathbf{4}) = \frac{1}{2}$ and $C(\mathbf{6}) = 1$. Below the scales M_1 and M_2, the numbers of right- and left-handed fermions are $n_{f_R} = n_{f_L} = 3$ because, per family, $(\mathbf{4}, \mathbf{1})_\mathbf{3}$ and $(\mathbf{4}^*, \mathbf{1})_{-\mathbf{3}}$ contribute one left-handed and one right-handed $\mathrm{SU}(4)_{\mathrm{DM}}$ fermion. When the M_1 scale is relevant, $(\mathbf{4}, \mathbf{1})_{-\mathbf{1}}$ of $\mathbf{6}$ of $\mathrm{SU}(6)$ contributes $(3+1)3 = 12$ to n_{f_L} and n_{f_R} since, per family, $(\mathbf{3}, \mathbf{1}, \mathbf{2}, \mathbf{1/6})_{L,R} + (\mathbf{3}, \mathbf{4}, \mathbf{1}, \mathbf{1/6})_{L,R}$ contributes 3 (due to color) and $(\mathbf{1}, \mathbf{1}, \mathbf{2}, -\mathbf{1/2})_{L,R} + (\mathbf{1}, \mathbf{4}, \mathbf{1}, -\mathbf{1/2})_{L,R}$ contributes 1. When M_2 is relevant, $(\mathbf{6}, \mathbf{2})_\mathbf{0}$ contributes 2 (due to the $\mathrm{SU}(2)_L$ doublet) per family to the number of left-handed fermions. The β-function for $\mathrm{SU}(4)_{\mathrm{DM}}$ is therefore $\beta_4(\alpha_4) = -f_4 \frac{\alpha_4^2}{2\pi}$, where

$$f_4^{\mu < M_1, M_2} = \left(\frac{11}{3} \cdot 4 - \frac{2}{3} \cdot \frac{1}{2} \cdot 3 - \frac{2}{3} \cdot \frac{1}{2} \cdot 3 \right) = \frac{38}{3},$$

$$f_4^{M_1 < \mu < M_2} = \left(\frac{11}{3} \cdot 4 - \frac{2}{3} \cdot \frac{1}{2} \cdot 3 - \frac{2}{3} \cdot \frac{1}{2} \cdot 3 - \frac{2}{3} \cdot \frac{1}{2} \cdot 12 - \frac{2}{3} \cdot \frac{1}{2} \cdot 12 \right) = \frac{14}{3} \quad (\text{when } M_1 < M_2),$$

$$f_4^{M_2 < \mu < M_1} = \left(\frac{11}{3} \cdot 4 - \frac{2}{3} \cdot \frac{1}{2} \cdot 3 - \frac{2}{3} \cdot \frac{1}{2} \cdot 3 - \frac{2}{3} \cdot 1 \cdot 6 \right) = \frac{26}{3} \quad (\text{when } M_2 < M_1),$$

$$f_4^{\mu > M_1, M_2} = \left(\frac{11}{3} \cdot 4 - \frac{2}{3} \cdot \frac{1}{2} \cdot 3 - \frac{2}{3} \cdot \frac{1}{2} \cdot 3 - \frac{2}{3} \cdot \frac{1}{2} \cdot 12 - \frac{2}{3} \cdot \frac{1}{2} \cdot 12 - \frac{2}{3} \cdot 1 \cdot 6 \right) = \frac{2}{3}. \tag{3.3}$$

Solving the β-function equation $\beta(\alpha) \equiv \frac{d\alpha}{d\ln\mu} = -f\frac{\alpha^2}{2\pi}$ gives us

$$\alpha(\mu_1)^{-1} = \alpha(\mu_2)^{-1} + \frac{f}{2\pi}\ln\frac{\mu_1}{\mu_2}. \tag{3.4}$$

Using equation (3.4) for $\mathrm{SU}(2)_L$ for different energy ranges and evaluating at μ_{DUT}, we get

$$\alpha_2(\mu_{\mathrm{DUT}})^{-1} = \alpha_2(\mu_{\mathrm{EW}})^{-1} + \frac{f_2^{\mu<M_2}}{2\pi}\ln\frac{M_2}{\mu_{\mathrm{EW}}} + \frac{f_2^{\mu>M_2}}{2\pi}\ln\frac{\mu_{\mathrm{DUT}}}{M_2}, \tag{3.5}$$

where $\mu_{\mathrm{EW}} = 246$ GeV is the electroweak energy scale, and $\alpha_2(\mu_{\mathrm{EW}}) \approx 0.03$. Using equation (3.4) for $\mathrm{SU}(4)_{\mathrm{DM}}$ for different energy ranges and evaluating at μ_{DUT} gives us

$$\alpha_4(\mu_{\mathrm{DUT}})^{-1} = \alpha_4(\mu_{\mathrm{DM}})^{-1} + \frac{f_4^{\mu<M_<}}{2\pi}\ln\frac{M_<}{\mu_{\mathrm{DM}}} + \frac{f_4^{M_<<\mu<M_>}}{2\pi}\ln\frac{M_>}{M_<} + \frac{f_4^{\mu>M_>}}{2\pi}\ln\frac{\mu_{\mathrm{DUT}}}{M_>}, \tag{3.6}$$

where μ_{DM} is the dark matter dynamical mass and $M_<$ $(M_>)$ is the lesser (greater) of M_1 and M_2. We assume that M_1 and M_2 are bigger than μ_{DM} and the electroweak scale or any observable scale. If M_1 or M_2 is on the order of μ_{DUT} (and therefore not affecting RG flow), one may set it equal to μ_{DUT} in equations (3.5) and (3.6) to get the appropriate expression. Using equations (3.5) and (3.6) and the unification of $\mathrm{SU}(2)_L$ and $\mathrm{SU}(4)_{\mathrm{DM}}$ at the DUT scale $(\alpha_4(\mu_{\mathrm{DUT}}) = \alpha_2(\mu_{\mathrm{DUT}}))$, we get an expression for the dark matter dynamical mass:

$$\mu_{\mathrm{DM}} = M_< \operatorname{Exp}\left[-\frac{2\pi}{f_4^{\mu<M_<}}(\alpha_2(\mu_{\mathrm{EW}})^{-1} - \alpha_4(\mu_{\mathrm{DM}})^{-1})\right]$$

$$\cdot \left(M_2^{f_2^{\mu>M_2}-f_2^{\mu<M_2}}\mu_{\mathrm{EW}}^{f_2^{\mu<M_2}}M_<^{-f_4^{M_<<\mu<M_>}}M_>^{f_4^{M_<<\mu<M_>}-f_4^{\mu>M_>}}\mu_{\mathrm{DUT}}^{f_4^{\mu>M_>}-f_2^{\mu>M_2}}\right)^{1/f_4^{\mu<M_<}}. \tag{3.7}$$

Essentially, we run the $\mathrm{SU}(2)_L$ gauge coupling from the known electroweak scale up to the DUT scale, which can be observationally constrained, and then we run the $\mathrm{SU}(4)_{\mathrm{DM}}$ gauge coupling down to its appropriate scale for dark matter. And the dark matter's dynamical mass should be approximately equal to the energy scale of confinement for $\mathrm{SU}(4)_{\mathrm{DM}}$, just as the major contribution to the quarks' masses comes mainly from the $\mathrm{SU}(3)_C$ confinement scale in the Standard Model. In figure 2, we show regions of confinement energy from $0.5 \leq \alpha_4 \leq 1.5$ for the one-loop RG flow for various values of μ_{DUT}, and we see that the variation in energy scale in these regions is not very significant. So we estimate that $\alpha_4(\mu_{\mathrm{DM}}) \sim 1$.

In preliminary analysis, we let M_2 vary from 10^5 GeV to μ_{DUT}, and we found that the dark matter dynamical mass was in general very high, ranging even up to 10^{13} GeV. Because we are not interested in such purely academic values of the dark matter dynamical mass, we assume $M_2 \sim \mu_{\mathrm{DUT}}$ in all our analysis that follows.

We emphasize the unique and interesting connection between the DUT scale and the dynamical mass of dark matter we have presented. This connection has been made independently of the model of inflation. In what follows, we specify an inflation model in order to apply inflation constraints from cosmological probes to μ_{DUT}.
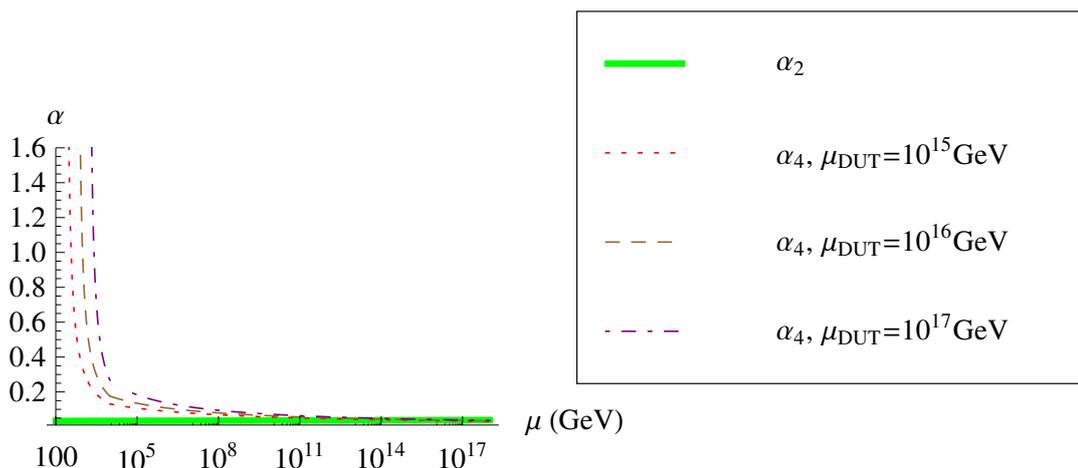
Figure 1. The unification of $SU(4)_{\text{DM}}$ and $SU(2)_L$ at the DUT scale for different values of μ_{DUT}. For these examples, we have chosen $M_1 = 10^4$ GeV and $M_2 \sim \mu_{\text{DUT}}$.
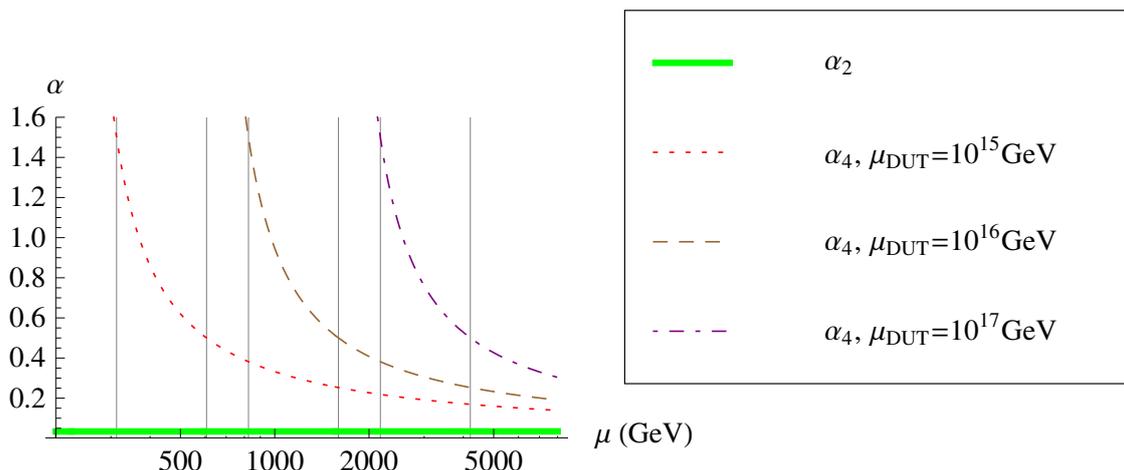

Figure 2. The regions of confinement for $0.5 \leq \alpha_4(\mu_{\text{DM}}) \leq 1.5$ for the functions from figure 1 with the same values for M_1 and M_2. The variation in energy scale in these regions is not very significant. We use $\alpha_4(\mu_{\text{DM}}) \sim 1$.

4   Constraints on inflation from Planck

As discussed in [2], the inflaton is expected to decay to dark matter during entropy generation after inflation. Using the slow-roll approximation, we examine a Coleman-Weinberg potential for inflation used in [8]:

$$V(\phi) = A(\phi + v)^4 \left[\ln \frac{(\phi + v)^2}{v^2} - \frac{1}{2} \right] + \frac{Av^4}{2}. \tag{4.1}$$

As in [8], ϕ can be thought of as the physical field that is the real part of a scalar field Φ such that $\Phi^\dagger \Phi = (\phi + v)^2$. The expectation value of ϕ is $\langle \phi \rangle = 0$, but $\langle \Phi \rangle = v$. So the potential
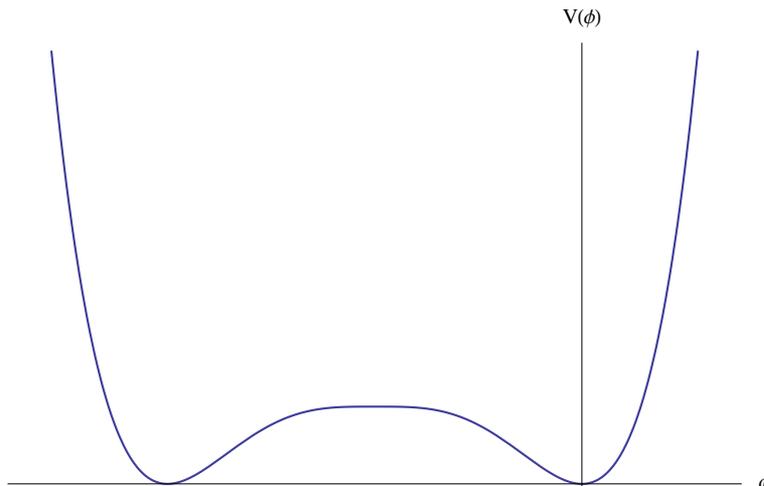
Figure 3. Our Coleman-Weinberg potential versus ϕ.

in terms of the full field Φ is this Coleman-Weinberg potential with $(\phi + v)^2 \to \Phi^\dagger \Phi$, and it has its local maximum centered around $\Phi = 0$, whereas the potential for ϕ has its local maximum centered around $\phi = -v$ (see figure 3). So we use the potential in terms of ϕ, which is mathematically equivalent up to a field shift of v, so the potential still displays the dynamics of a Coleman-Weinberg potential.

The phase transition into the true vacuum energy with $\langle \Phi \rangle = v$ will provide the symmetry breaking needed for the breaking of $\mathrm{SU}(6) \to \mathrm{SU}(4)_{\mathrm{DM}} \times \mathrm{SU}(2)_L \times \mathrm{U}(1)_{\mathrm{DM}}$. So we expect $\mu_{\mathrm{DUT}} = v$, and we constrain v using inflation constraints from Planck.

Two significant constraints from Planck [6, 7], assuming no running of the scalar spectral index and no tensor perturbations, come from the scalar spectral index, $n_s(k_\star) = 0.9603 \pm 0.0073$, and the scalar power-spectrum amplitude $A_s(k_\star)$, $\ln(10^{10} A_s(k_\star)) = 3.089^{+0.024}_{-0.027}$. These values come from temperature power spectrum data from Planck and WMAP polarization at low multipoles and are obtained at the pivot scale $k_\star = 0.05 \ \mathrm{Mpc}^{-1}$, and the scalar power spectrum with no running is modeled as $\mathcal{P}_s(k) = A_s(k_\star) \left(\frac{k}{k_\star}\right)^{n_s - 1}$. When tensor perturbations are considered with no running of the scalar or tensor spectral indexes, Planck reports at the 95% confidence level $r(k_\star) \equiv \frac{A_s(k_\star)}{A_t(k_\star)} < 0.12$ for the tensor-scalar ratio and $n_s(k_\star) = 0.9624 \pm 0.0075$ using the same data sources mentioned earlier and obtained at the pivot scale $k_\star = 0.002 \ \mathrm{Mpc}^{-1}$. We note that the latest joint analysis of the Planck and BICEP2/Keck data [9] overturn BICEP2's high estimate of r, which we do not consider in our analysis. Although Planck also gives constraints on slow-roll parameters of higher order when running is allowed, depending on the data set used, they are consistent with no running and are not very helpful in constraining our model, so we do not present analysis concerning these constraints from Planck here.

We use the slow-roll approximation to first order to apply these constraints, and we evaluate at the pivot scale's Hubble radius crossing, which is denoted by $\star$ as a superscript or subscript. Natural units are used throughout with the reduced Planck mass $M_{\mathrm{Pl}} \equiv (8\pi G)^{-1/2}$.

The scalar spectral index at the pivot scale in terms of the slow-roll potential parameters is given by

$$n_s(k_\star) = 1 + 2\eta_V^\star - 6\epsilon_V^\star, \tag{4.2}$$

where

$$\epsilon_V = \frac{M_{\rm Pl}^2}{2} \left(\frac{V_{,\phi}}{V} \right)^2 \tag{4.3}$$

and

$$\eta_V = M_{\rm Pl}^2 \frac{V_{,\phi\phi}}{V}. \tag{4.4}$$

The scalar power spectrum amplitude is given by

$$A_s(k_\star) = \frac{1}{24\pi^2} \frac{V_\star}{M_{\rm Pl}^4} \frac{1}{\epsilon_V^\star}, \tag{4.5}$$

the tensor-scalar ratio at the pivot scale is

$$r(k_\star) = 16\epsilon_V^\star, \tag{4.6}$$

and the number of e-folds before the end of inflation when the pivot scale $k_\star$ exited the Hubble radius, $N_\star$, is given by

$$N_\star = \frac{1}{M_{\rm Pl}^2} \int_{\phi_{\rm end}}^{\phi_\star} \frac{V}{V_{,\phi}}. \tag{4.7}$$

Plugging in our potential from equation (4.1) into equation (4.2), we obtain the relation

$$\begin{aligned}
v^2 \; (n_s(k_\star) - 1)[x_\star(4 + 6x_\star + 4x_\star^2 + x_\star^3) - 2(1 + x_\star)^4 \ln(1 + x_\star)^2]^2 = \\
16M_{\rm Pl}^2 \; (1 + x_\star)^2[(4 + 4x_\star + 6x_\star^2 + 4x_\star^3 + x_\star^4) \ln(1 + x_\star)^2 \\
- 6(1 + x_\star)^4[\ln(1 + x_\star)^2]^2 - 2x_\star(4 + 6x_\star + 4x_\star^2 + x_\star^3)],
\end{aligned} \tag{4.8}$$

where $x \equiv \frac{\phi}{v}$. In our potential in figure 3, the domain of inflation begins soon after (to the right of) the local maximum at $\phi = -v$ (or $x = -1$), and we determine $x_{\rm end}$ from the condition $\epsilon_V = 1$, which is when the acceleration of the universe due to inflation ceases, and this happens before entropy generation around the local minimum at the origin.

Using equations (4.2) and (4.5), we get

$$V_\star^3 = 192 \; M_{\rm Pl}^6 \; \pi^2 \; A_s(k_\star) \; (1 + x_\star)^6 \; [\ln(1 + x_\star)^2]^2 \; v^6. \tag{4.9}$$

Evaluating the definite integral in equation (4.7), we get

$$\begin{aligned}
N_\star = -\frac{v^2}{16M_{\rm Pl}^2} \{ 2(x_\star - x_{\rm end})(x_\star + x_{\rm end} - 34) + {\rm Ei}[-\ln(1 + x_\star)^2] \\
- {\rm Ei}[-\ln(1 + x_{\rm end})^2] - {\rm li}[(1 + x_\star)^2] + {\rm li}[(1 + x_{\rm end})^2] \},
\end{aligned} \tag{4.10}$$

where ${\rm li}(y) \equiv \int_0^y \frac{ds}{\ln s}$ and ${\rm Ei}(y) \equiv \int_{-y}^\infty \frac{e^{-s}}{s} ds$.

Comparing equations (4.8) and (4.9) with the aforementioned constraints from Planck on n_s and A_s, $v = \mu_{\rm DUT}$ is given below for reasonable choices of the energy scale of inflation, $V_\star^{1/4}$.

$V_\star^{1/4} = 10^{13}\,{\rm GeV}, \quad A = (8.837 \pm 1.563)\,10^{-6}, \quad v = (2.192 \pm 0.098)\,10^{14}\,{\rm GeV}, \quad N_\star = 79.25 \pm 14.57$

$V_\star^{1/4} = 10^{14}\,{\rm GeV}, \quad A = (9.422 \pm 1.669)\,10^{-6}, \quad v = (2.157 \pm 0.096)\,10^{15}\,{\rm GeV}, \quad N_\star = 79.49 \pm 14.61$

$V_\star^{1/4} = 10^{15}\,{\rm GeV}, \quad A = (1.021 \pm 0.181)\,10^{-5}, \quad v = (2.114 \pm 0.095)\,10^{16}\,{\rm GeV}, \quad N_\star = 79.88 \pm 14.68$

$V_\star^{1/4} = 10^{16}\,{\rm GeV}, \quad A = (1.136 \pm 0.202)\,10^{-5}, \quad v = (2.059 \pm 0.093)\,10^{17}\,{\rm GeV}, \quad N_\star = 80.63 \pm 14.80$

$V_\star^{1/4} = 10^{17}\,{\rm GeV}, \quad A = (1.336 \pm 0.240)\,10^{-5}, \quad v = (1.977 \pm 0.090)\,10^{18}\,{\rm GeV}, \quad N_\star = 83.80 \pm 15.26\,.$

$$\tag{4.11}$$

Scenario	DM Mass for $\mu_{\mathrm{DUT}} = 10^{18}\,\mathrm{GeV}$	DM Mass for $\mu_{\mathrm{DUT}} = 10^{14}\,\mathrm{GeV}$
$M_1 \sim \mu_{\mathrm{DUT}}$	4.7×10^{12}	2.9×10^{8}
$M_1 = 10^{17}\,\mathrm{GeV}$	1.1×10^{12}	—
$M_1 = 10^{16}\,\mathrm{GeV}$	2.6×10^{11}	—
$M_1 = 10^{15}\,\mathrm{GeV}$	6.0×10^{10}	—
$M_1 = 10^{14}\,\mathrm{GeV}$	1.4×10^{10}	—
$M_1 = 10^{13}\,\mathrm{GeV}$	3.3×10^{9}	6.8×10^{7}
$M_1 = 10^{12}\,\mathrm{GeV}$	7.6×10^{8}	1.6×10^{7}
$M_1 = 10^{11}\,\mathrm{GeV}$	1.8×10^{8}	3.7×10^{6}
$M_1 = 10^{10}\,\mathrm{GeV}$	4.2×10^{7}	8.6×10^{5}
$M_1 = 10^{9}\,\mathrm{GeV}$	9.7×10^{6}	2.0×10^{5}
$M_1 = 10^{8}\,\mathrm{GeV}$	2.3×10^{6}	4.7×10^{4}
$M_1 = 10^{7}\,\mathrm{GeV}$	5.3×10^{5}	1.1×10^{4}
$M_1 = 10^{6}\,\mathrm{GeV}$	1.2×10^{5}	2.6×10^{3}
$M_1 = 10^{5}\,\mathrm{GeV}$	2.9×10^{4}	6.0×10^{2}
$M_1 = 10^{4}\,\mathrm{GeV}$	6.8×10^{3}	1.4×10^{2}

Table 3. Upper and lower bounds on dark matter dynamical mass derived from a range of μ_{DUT} from equation (4.11) for various scenarios (with $M_2 \sim \mu_{\mathrm{DUT}}$). Values are only provided for scenarios in which $M_1 \lesssim \mu_{\mathrm{DUT}}$. All values are given in GeV. The small value of the dark matter dynamical mass lower bound on the last row is given without concern for the phenomenological constraints on mirror-fermion masses, which are discussed in [10].

Using these results and equation (4.6), we find that $r \lesssim 10^{-8}$ for all these scenarios, so Planck's constraint on r is satisfied. The precise value of $N_\star$ depends on the energy scale of inflation and the uncertain details of entropy generation at the end of inflation (see, for example, equation (24) of [7] for more details), but the value of $N_\star$ for each scenario above is greater than the minimum number required to solve the horizon problem for each energy scale.

The constrained values of μ_{DUT} in equation (4.11) imply values for dark matter dynamical mass depending on what M_1 and M_2 are. The values of $v = \mu_{\mathrm{DUT}}$ in equation (4.11) range from 10^{14}–$10^{18}\,\mathrm{GeV}$. In table 3, using equation (3.7) for various scenarios concerning the choice of M_1, we give the upper and lower bounds for dark matter dynamical mass based on this range for μ_{DUT}. A wide range of predictions of dark matter dynamical mass is exemplified in figure 4 for various scenarios. There are no strong astrophysical constraints on the scale of M_1, and the number density of these particles is in general below a detectable level due to Boltzmann suppression. In fact, we even show scenarios in which M_1 is as low as $10^4\,\mathrm{GeV}$ since the Boltzmann suppression factor ($e^{-M/T}$) in the number density for particles of mass $10^4\,\mathrm{GeV}$ in equilibrium would be e^{-100} and stronger for temperatures of $T \sim 100\,\mathrm{GeV}$ (electroweak scale) and lower. Since a candidate for dark matter with moderately low mass is in general desirable, we show that such a dynamical mass is attainable with the appropriate choice of M_1. If or when the dark matter mass is more precisely constrained in the future, we can then know what the scale of M_1 is. M_1 particles could be produced in high-energy astrophysical phenomena such as active galactic nuclei or quasars, and they would annihilate
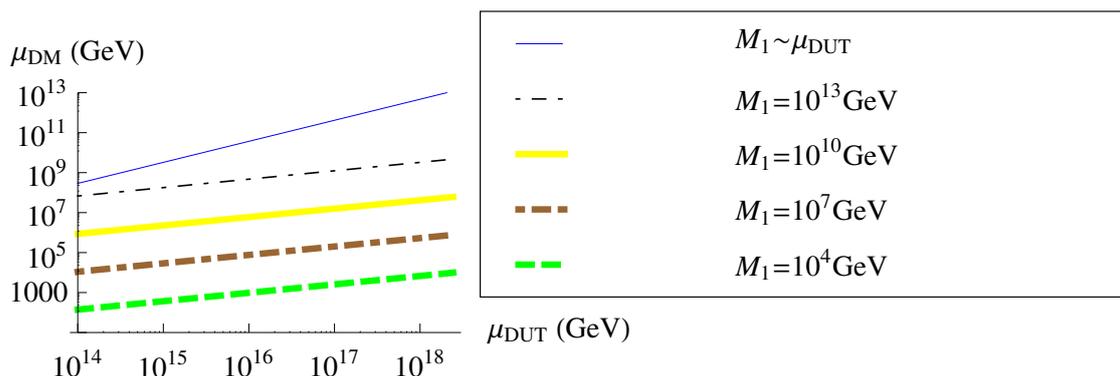
$\mu_{\rm DM}$ (GeV)

10^{13}
10^{11}
10^{9}
10^{7}
10^{5}
1000

10^{14} 10^{15} 10^{16} 10^{17} 10^{18}

$\mu_{\rm DUT}$ (GeV)

$M_1 \sim \mu_{\rm DUT}$

$M_1 = 10^{13}\,$GeV

$M_1 = 10^{10}\,$GeV

$M_1 = 10^{7}\,$GeV

$M_1 = 10^{4}\,$GeV

Figure 4. $\mu_{\rm DM}$ is shown for a few chosen scenarios (with $M_2 \sim \mu_{\rm DUT}$).

into radiation detected on Earth. We could constrain the cross section of such particles once the scale of M_1 is deduced from the mass of dark matter. Note that the inflaton, with mass $m_\phi = \sqrt{8A}v$, decays to two dark matter particles, which are massless until the confinement scale $\mu_{\rm DM} \ll \mu_{\rm DUT}$.

5 Conclusion

In this paper, we explore the unique connection in the luminogenesis model, a model that consistently combines dark matter and the Standard Model, between cosmic inflation and the creation of dark matter that allows the constraining of the dynamical mass of dark matter particles. The constraint on $\mu_{\rm DUT}$ is obtained by fitting a particular symmetry-breaking potential, although the connection between the unification scale $\mu_{\rm DUT}$ and the dark matter dynamical mass $\mu_{\rm DM}$ remains independent of the supposed correct model of inflation.

Since the descent into the true vacuum of inflation triggers the breaking of the DUT symmetry and thus the conversion of the inflaton to dark matter, we can arrive at rough constraints on the DUT scale via constraints on inflation from cosmological probes. Through picking a Coleman-Weinberg potential and reasonable energy scales for inflation, we arrive at constraints on the DUT scale, and we can then derive an upper bound on the dark matter dynamical mass via RG flow. We run the $SU(2)_L$ coupling from the known electroweak scale up to the DUT scale, where it is unified with $SU(4)_{\rm DM}$. We then run the $SU(4)_{\rm DM}$ coupling down to its confinement scale, taken to be when $\alpha_4 \sim 1$, and we arrive at the dynamical mass scale for dark matter. Various dynamical mass values for dark matter are possible depending on the mass scale M_1 and M_2. The possibility of strongly self-interacting dark matter, as proposed in [1, 2], with dynamical masses obtained through the connection $\mu_{\rm DUT} \to \mu_{\rm DM}$ as studied here has wide implications concerning the resolution of dwarf galaxy structures and dark matter cusps at the centers of galaxies and its potential detectability. This is under investigation.

Acknowledgments

References

[1] P.H. Frampton and P.Q. Hung, *Positron Excess, Luminous-Dark Matter Unification and Family Structure*, *Phys. Lett.* **B 675** (2009) 411 [`arXiv:0903.0358`] [INSPIRE].

[2] P.H. Frampton and P.Q. Hung, *Luminogenesis from Inflationary Dark Matter*, `arXiv:1309.1723` [INSPIRE].

[3] P.Q. Hung, *A Model of electroweak-scale right-handed neutrino mass*, *Phys. Lett.* **B 649** (2007) 275 [`hep-ph/0612004`] [INSPIRE].

[4] V. Hoang, P.Q. Hung and A.S. Kamat, *Electroweak precision constraints on the electroweak-scale right-handed neutrino model*, *Nucl. Phys.* **B 877** (2013) 190 [`arXiv:1303.0428`] [INSPIRE].

[5] S. Chakdar, K. Ghosh, V. Hoang, P.Q. Hung and S. Nandi, *The search for mirror quarks at the LHC*, `arXiv:1508.07318` [INSPIRE].

[6] PLANCK collaboration, P.A.R. Ade et al., *Planck 2013 results. XVI. Cosmological parameters*, *Astron. Astrophys.* **571** (2014) A16 [`arXiv:1303.5076`] [INSPIRE].

[7] PLANCK collaboration, P.A.R. Ade et al., *Planck 2013 results. XXII. Constraints on inflation*, *Astron. Astrophys.* **571** (2014) A22 [`arXiv:1303.5082`] [INSPIRE].

[8] P.Q. Hung, E. Massó and G. Zsembinszki, *Low-scale inflation in a model of dark energy and dark matter*, *JCAP* **12** (2006) 004 [`astro-ph/0609777`] [INSPIRE].

[9] BICEP2, PLANCK collaboration, P. Ade et al., *Joint Analysis of BICEP2/KeckArray and Planck Data*, *Phys. Rev. Lett.* **114** (2015) 101301 [`arXiv:1502.00612`] [INSPIRE].

[10] V. Hoang, P.Q. Hung and A.S. Kamat, *Non-sterile electroweak-scale right-handed neutrinos and the dual nature of the 125-GeV scalar*, *Nucl. Phys.* **B 896** (2015) 611 [`arXiv:1412.0343`] [INSPIRE].